Simultaneous optical and electrical mixing in a single fast photodiode for the demodulation of weak mm-wave signals

Michele Norgia, Guido Giuliani, Riccardo Miglierina and Silvano Donati
University of Pavia, Pavia, Italy
Tiziana Tambosso
Telecom Italia Lab, Torino, Italy

ABSTRACT

In this work we demonstrate that the normal photomixing scheme, i.e. one built around a two-mode laser (or a mode-locked laser) as the source, and a fast photodiode acting as the optical mixer of the two modes, can be used also to perform the electrical demodulation of an incoming weak signal at the same frequency.
In particular, we consider a mode spacing c/2L in the range of mm-waves, typically 60GHz for a practical WLAN communication system. With optical powers in the range of mW's (or 0dBm) for each mode, and an optical power amplifier boosting powers up to 8-10 dBm, the two modes can be photomixed on a high frequency photodiode and obtain an electrical signal with power of about 0dBm at the carrier frequency of 60GHz. Now, if an electrical signal, with a frequency slightly different from 60GHz, is applied to the photodiode output, electrical mixing with the photomixing carrier takes place and demodulation of the weak signal is performed, down to the baseband.

Keywords: Photomixing, demodulation, mm-waves

1. INTRODUCTION

Recently, generation of mm-waves by photomixing has attracted great interest because of the potentiality in broadband communication at both 60 and 72 GHz, such as high-speed wireless LAN, fixed wireless access (FWA), and in-house wide-band signal broadcasting [1-4]. Photomixing is a well-known and mature technique for the generation of clean local oscillators in radio astronomy [5], and for the conversion from mode-locked ultrafast optical pulses to THz waves in the so-called T-Ray imaging.

In communications, it is appealing because it may provide a completely new approach for the generation of mm-wave frequencies, alternative to conventional microwave techniques and potentially more flexible and low-cost. In the last years, much research has been devoted to demonstrate photomixing generators with a narrow-line carrier and low phase-noise, such as required by modern modulation techniques [1], and that this can be done with a relatively simple stabilization or frequency-locking scheme easy to be incorporated in the basic photomixing structure.

On the other hand, in the roadmap of achieving low-cost, integrated transceivers for application to broadband communications at 60-72 GHz, an important step is to define which components are best suited to implement photomixing in integrated technology. Thus, for the laser, we have either the Fabry-Perot linear and ring cavity [6,7] or the DBR [8,9] options, then we shall manage back-reflections in the MOPA (master oscillator power amplifier) structure, and finally, shall optimize the photodiode for bandwidth and saturation current [10].

A seminal work on the integration of three basic elements of the photomixing generator is provided by the paper of Vawter et al. [11]. They have integrated, in GaAs/AlGaAs technology, a ring laser, an optical amplifier and a co-planar wave-guide photodiode. The ring laser was fabricated in three sizes, 860, 430 and 290μm diameter for a mode spacing of 30, 60 and 90 GHz. Mode locking was achieved by reverse-biasing a short (~50μm) section of the active ring guide. The ring laser output was coupled through a Y-guide coupler to an optical amplifier a few mm long that provides a gain of about 8 dB. The optical amplifier ended on a waveguide photodiode with co-planar electrical output. The

electrical powers obtained from this integrated photomixing generator were modest, i.e., -12, -23 and -27dBm at the three frequencies, respectively; with an unexpected roll-off probably due to the non-insulating substrate used in fabrication. Yet the result was important because it was probably the first example of mm-wave generation with a compact (<1mm) semiconductor device other than conventional microwave components.

However, several issues shall be taken into account if we are to develop the concept of integrated photomixing further, and be able to approach a device of practical importance. First, at the device level, we need substantially to improve the powers generated by the MOPA and converted by the photodiode into mm-wave power, as system studies indicate that at least 0 to +5 dBm should be fed to the antenna in a reasonable short-range communication link. Second, at the level of functions performed, we shall envisage adequate means to modulate intelligence on the generated mm-wave carrier, as well as to demodulate the intelligence in the mm-wave signal received by the antenna.

Modulation can be performed either on the source, using the current-to-wavelength dependence to impress frequency modulation, but with a limited bandwidth (up to MHz), or through the optical-amplifier bias-current, thus resulting in an amplitude modulation that may encompass several hundreds MHz or a GHz. Still higher modulation bandwidth could be obtained if we are willing to add a electro-absorption modulator (EAM) among the optical signal path from amplifier to photodiode.

About demodulation, we can of course use a duplicate of the photomixing generator to obtain the local oscillator that need to be superposed in a conventional diode-mixer to the signal received by the antenna. But, much better, we may try to perform the electrical mixer function already at the photodiode itself, taking advantage from the presence at the photodiode of the mm-wave carrier generated by the photomixing process [12].

As there is no reason to think that the photomixing photodiode is a bad electrical mixer, as a first step we try to validate the idea of the simultaneous optical and electrical mixing in a single fast photodiode, as it is presented in Sect.2. In Sect.3, we will report a few simulations confirming the demodulation effect shown by experimental results.

For the results to be meaningful, we have used discrete devices, that are however similar in structure and performance to those that can be designed and fabricated in an integrated chip.

As a general comment, the double mixing process saves components and chip area, but introduces a system constraint to the operation of the transceiver: in fact, in order to have an unmodulated carrier for reception, the modulation of the transmitter shall be switched off while receiving, which means that the device works in half-duplex.

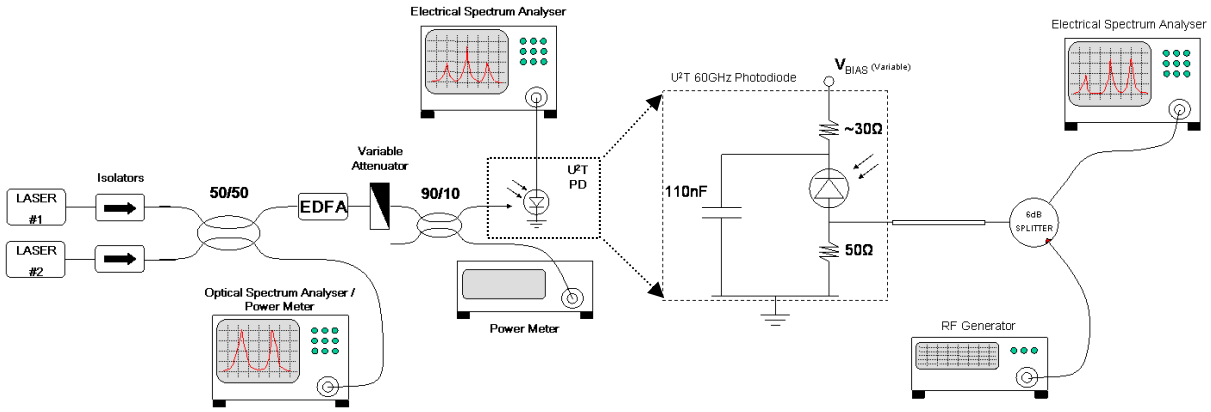

Figure 1. Basic scheme of the double-mixing experiment.

2. EXPERIMENT

The setup used to experiment with the double-mixing arrangement is shown in Fig.1. We use two CW laser sources (Lasers #1 and #2), a DFB laser fabricated by CSELT with a Peltier temperature controller, and a commercial tunable laser from Photonetics, both working in the communications third-window. The relative frequency difference of the two sources is stable within ~1 MHz, as seen from the beating output at low frequency observed at the electrical spectrum analyzer (ESA), and can be finely tuned either by changing DFB laser temperature and current or by controlling tunable laser wavelength. Two optical isolators are introduced to prevent optical power back-injection, which may lead to laser instability or chaos. A 50/50 single-mode fiber coupler is used to overlap the two optical signals: one of the two output fibers is connected to an optical spectrum analyzer (OSA), which allows to coarsely control the frequency difference of two optical lines with a resolution of about 12.5GHz (this limitation is due to OSA optical resolution of 0.1nm). The other coupler output fiber is then connected to a 60GHz U^2T waveguide photodiode, which acts as the optical mixer (i.e. photomixer) detecting the power of the sum of the two lasers signals, and thus generating the electrical beat between the two optical lines. Now, connecting the photodiode output to an the electrical spectrum analyzer, we can finely measure the frequency of this beat signal (i.e. the frequency difference between the two lasers) with a resolution of about 100kHz (i.e. ESA resolution bandwidth). In order to boost up the optical power (thus increasing the electrical beat signal power), we add to the experimental setup an erbium-doped fiber amplifier and an optical variable attenuator: besides, a 90/10 coupler is necessary to monitor the actual optical power injected in the photodiode.

After generating the photomixing signal, which will act as the local oscillator (LO) signal, we now need to simulate the presence of the electrical signal received by the antenna and apply it to the photodiode output; for this reason, we introduce in our setup a 40GHz RF electrical signal generator, which is used to generate an RF sinusoidal signal with a frequency that is slightly different (i.e. from 500MHz to 5GHz) from photomixing LO frequency. Because of the photodiode electrical nonlinearities (both resistive and capacitive), electrical mixing takes place between the LO photomixing signal and the simulated antenna signal, thus generating an electrical beat signal (i.e. down-conversion of the antenna electrical signal) over the photodiode output, with a frequency value equal to the frequency difference between the two input electrical signals. In summary, looking at the whole conversion process, the high-bandwidth photodiode acts as a double-mixer (i.e. both optical and electrical).

As we need to measure the amplitude and frequency of all the electrical signals (LO, antenna and down-conversion) through the ESA, the RF generator connection to the photodiode output is made through a 6dB power divider, as shown in Fig. 1. This device represents the only true frequency limitation of our setup; in fact, the 6dB splitter we used for all measurements was characterized by a bandwidth of about 12.4GHz. After a calibration procedure through a conventional network analyzer, we were able to extend this frequency range up to a maximum value of 35GHz; so, all experimental results we present in this paper are relative to electrical signals with a frequency value smaller than 35GHz only because of the 6dB splitter bandwidth limitation.

The main parameter we want to estimate is the conversion loss CL (expressed in dB); this value, which determines the efficiency of the electrical-mixing phenomenon, is defined by the equation:

$$CL\big|_{dB} = \frac{P_{PMIX}\big|_{dBm} + P_{RF}\big|_{dBm}}{2} - P_{CONV}\big|_{dBm}$$

where P_{PMIX} and P_{RF} are, respectively, the photomixing signal electrical power and the RF generator signal power, while P_{CONV} is the power of the down-converted signal (i.e. with a frequency equal to the frequency difference of the two input signals). The first set of measurements of the conversion loss was executed by keeping the frequency difference between the LO and antenna signal at a constant value of about 1GHz (i.e. maintaining constant the down-conversion signal frequency), while sweeping the mean value of the two input signals frequency from 5 to 35GHz. The powers of all the three signals were measured on the ESA and then, using the power divider calibration data, all measures were back-propagated to the effective power values measured directly on the photodiode output. Finally, in order to maximize the down-converted signal power, it is also important to control the photodiode reverse voltage; for this reason, all measurements were repeated for four different photodiode polarization voltage values: 2V, 1.5V, 400mV and -400mV (i.e. small direct voltage). All this experimental results are shown in Figure 2; during all measures, the RF generator signal and the photomixing LO signal powers were kept constant respectively at +10dBm and -10dBm.

Figures 2a and 2b show the effective electrical power of the RF generator signal and of the photomixing signal, as measured at the photodiode output. The RF signal power variation with frequency (shown in Figure 2a) is mainly caused by the power divider transmission coefficient frequency response; on the other side, the photomixing power variation shown in Figure 2b is due to electrical impedance mismatch. Moreover, the photomixing signal fades at -400mV because of the photodiode responsivity decrease due to direct polarization.

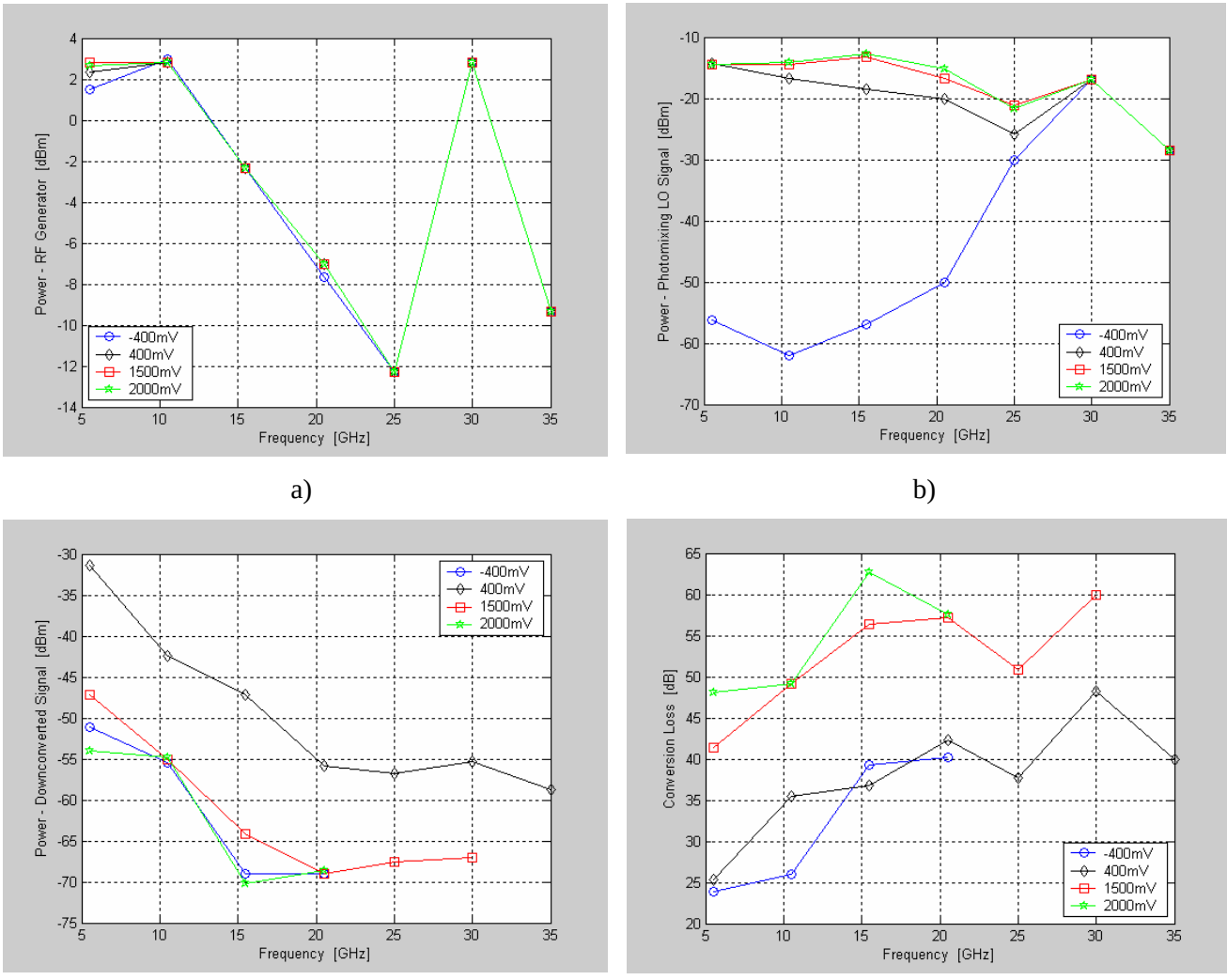

Figure 2. Double-mixing conversion loss characterization measures, executed for four different photodiode reverse voltage values (2V, 1.5V, 400mV and -400mV) while keeping constant the frequency difference between the RF generator signal and the photomixing-generated signal and sweeping the two input signals frequency mean value from 5 to 35GHz: a) RF generator signal power, b) photomixing signal power, c) frequency difference signal power and d) conversion loss. All measures are relative to the actual power measured at the photodiode output.

In Figures 2c and 2d we can observe, respectively, the dependence of the down converted signal power on the mean frequency value of the two input signals and the estimated conversion loss, as defined in the above equation. The electrical mixing efficiency is maximized (i.e. minimum of the conversion loss, 25dB) at a reverse voltage value of about 400mV and it decreases with an increase of the frequency of the RF and photomixing signals. This decrease can be explained in two ways:

1. The electrical mixing efficiency is strictly connected to photodiode resistive and capacitive nonlinearities, which may be characterized by a frequency cut-off;

2. During all measures, we observed a strong dependence of the down-converted signal power on the photomixing signal power variations. As visible in Figures 2b, variations of 5 to 10dB in the photomixing signal occur within the 5-25GHz frequency range; this should cause the strong decrease of the conversion loss we observe in Figure 2c in the same frequency range.

To understand the real motivation of this efficiency decrease, it is necessary to simulate an accurate model of the double-mixing phenomenon, taking into account the frequency response effects of the photodiode nonlinear coefficients (see Section 3).

We also measured the dependence of the down-converted signal power on the frequency difference between the two input signals. This measurement is very important because it determines the available modulation bandwidth that can be carried by the RF antenna signal, as allowed by the double-mixing detection arrangement. The measurement procedure consists in keeping constant the photomixing signal frequency at a value of 10GHz and sweeping the RF signal frequency from 5.5 to 9.5GHz, thus obtaining a down-converted signal frequency varying from 500MHz to 4.5GHz. During the whole process, the power of the two input signals is kept constant to the values previously chosen for the constant frequency difference measures (RF generator +10dBm, photomixing -10dBm). All measures were repeated for four different values of photodiode reverse voltage; the results of these experiment are shown in Figure 3.

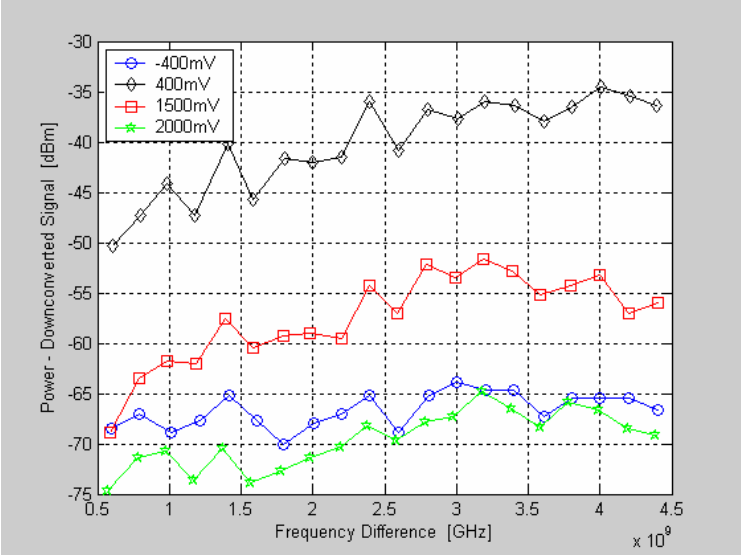

Figure 3. Down-converted signal power dependence on the frequency difference between the RF and photomixing input signals, measured for four different photodiode reverse voltage values. The experiment was executed by keeping constant the RF generator signal frequency at 10GHz while sweeping the photomixing signal frequency from 5.5 to 9.5GHz, thus obtaining a characterization of the down-converted signal in the 500MHz-4.5GHz frequency range.

Despite of power variations due to electrical mismatching, the down-converted signal show very little power variations (i.e. of the order of a few dBs); besides, the maximum signal power is obtained for a reverse voltage of about 400mV, in good agreement with what we observed in constant frequency difference measures (see Figure 2). As no major frequency cut-off was revealed, we can conclude that the double-mixing technique using the setup shown in Figure 1 allows a modulation bandwidth not smaller than 4.5GHz.

3. THEORETICAL EVALUATION

We have performed a simple calculation of the theoretical efficiency of down-conversion, based on a small signal nonlinear circuit model of the setup shown in Figure 1; we use a photodiode model that accounts for the first and second order coefficient of the I-V characteristics, both in the resistance component as well as in the capacitance component, and for simplicity we omit to simulate the presence of the 6dB power divider. In our model, the two fitting parameters, which are responsible for the frequency down-conversion process, are the second derivatives of the photodiode I-V curve and junction capacitance; the other parameters (i.e. RF generator and photomixing signal input powers, photodiode model linear coefficients, etc.) has been measured during the experiments or calculated using the conventional Shockley diode model.

In Figures 4 and 5 we show the simulation results obtained by applying a 5GHz RF generator signal with an electrical power of about +10dBm and a 6GHz photomixing signal with a power of about -10dBm. Figure 4 shows the time-domain evolution of the photodiode output voltage, while Figure 5 shows the power spectrum of the same signal.

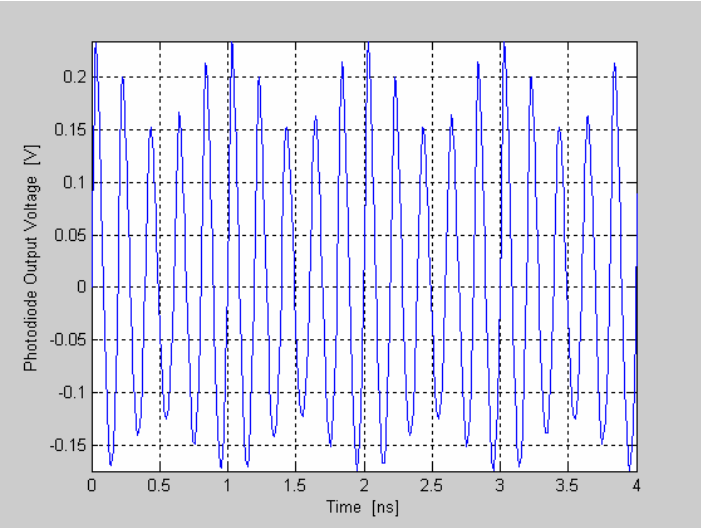

Figure 4. Simulation results of a nonlinear small signal model of the double-mixing arrangement shown in Figure 1: time-domain evolution of the photodiode output voltage, applying a 5GHz RF generator signal with an electrical power of about +10dBm and a 6GHz photomixing signal with a power of about -10dBm.

Figure 4 shows the typical time evolution of the signal given by the linear superposition of two sine signals with different frequency; the amplitude modulation frequency is 1GHz, which corresponds to the actual frequency difference between the two input signals. To reveal the presence of the electrical nonlinear beat signal and to measure the conversion loss, it is necessary to observe the power spectrum obtained via FFT elaboration, as shown in Figure 5. The signal spectrum has a 1GHz component with amplitude of -50dBm, corresponding to the down-converted signal. Using the conversion loss equation given in Section 2, the calculated conversion efficiency is of around 34dB; this value is in

good agreement with the measured conversion loss relative to the case of a 400mV photodiode reverse voltage (see Figure 2d). We have to remark that the conversion loss value depends dramatically on the nonlinear capacitive effect, which is the dominating fitting parameter of our model.

4. CONCLUSIONS

The experimental results (see Section 2) about the double-mixing phenomenon efficiency show that the setup reported in Figure 1 is a good solution both for mm-wave generation (through the photomixing technique) and for mm-wave electrical demodulation, using the same device (i.e. high-bandwidth photodiode) for the two frequency conversion processes. The maximum photomixing-generated electrical power is limited only by photodiode electrical saturation power (in our case ~0dBm); on the other side, we experimentally demonstrated a maximum electrical down-conversion efficiency of about 25dB, mainly depending on photodiode capacitive nonlinearity. Numerical simulations based on a simple model of the double-mixing arrangement have been carried out, showing a good agreement with the experimental results.

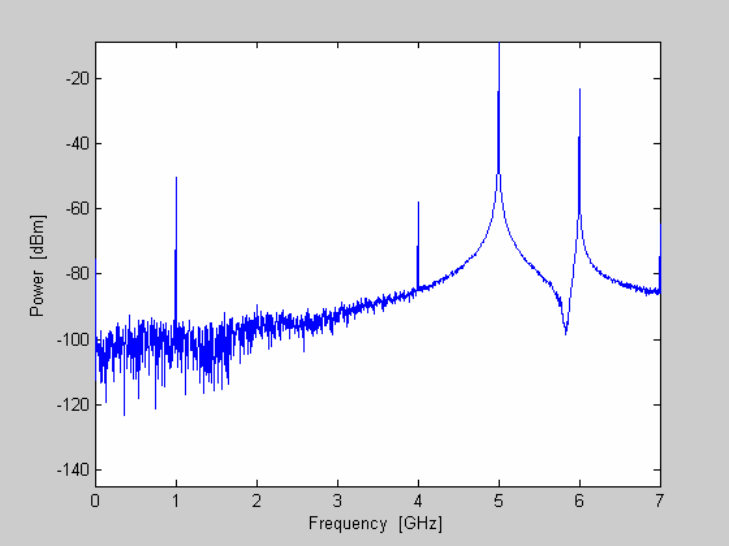

Figure 5. Simulation results of a nonlinear small signal model of the double-mixing arrangement shown in Figure 1: FFT power spectrum of the photodiode output voltage (see Figure 4). The signal spectrum shows a -50dBm 1GHz component, corresponding to the down-converted signal; the theoretical conversion loss is of about 34dB.

REFERENCES

1. Y. Shoji, K. Hamaguchi, H. Ogawa: “Millimeter Wave Remote Self-Heterodyne System for Extremely Stable and Low-Cost Broad-Band Signal Transmission”, IEEE Trans on Microw. Theory and Techn., vol.50 (2002), pp.1458-1467.
2. T.Kuri, K.Kitayama, A.Stohr, Y.Ogawa: "Fiber-Optic Millimiter-Wave Downlink System using 60GHz-Band External Modulation, IEEE J. Lightw. Techn., vol.17 (1999), pp.799-806.

3. R.P. Braun, G. Grosskopf, et al.: "Optical Microwave Generation and Transmission Experiment in the 12- and 60GHz Region for Wireless Communications", IEEE Trans. on Microw. Theory and Techn., vol.46, (1998), pp. 320-330.
4. R.P. Braun et al., "Optical Microwave Generation and Trasmission Experiment in the 12- and 60-GHz Region for Wireless Communications", IEEE Trans. on Microw. Theory and Techn., vol.46, (1998), pp. 320-330.
5. see the ALMA 400-papers literature at www.mma.nrao.edu/memos/html-memos
6. M. Sorel, P. Laybourn, A. Scirè, S. Balle, G. Giuliani, S. Donati: "Alternate Oscillations in Semiconductor Ring Laser", Optics Lett., vol.27 (2002), pp.1992-1994.
7. M.Sorel, G.Giuliani, A. Scirè, R.Miglierina, S.Donati, P. J. R.Laybourn: "Operating Regimes of GaAs–AlGaAs Semiconductor Ring Lasers: Experiment and Model" IEEE J. Quantum Electron., vol.39, (2003), pp.1187-95
8. D. Wake, C.R.Lima, P.A.Davies: "Optical Generation of Millimeter-Wave Signals for Fiber-Radio Sistems using a Dual-Mode DFB Semiconductor Laser", IEEE Trans. on Microw. Theory and Techn., vol.43, (1995), pp. 2270-2276.
9. G. Großkopf, D. Rohde, R. Eggemann, S. Bauer, C. Bornholdt, M.Mohrle, B. Sartorius, "Optical Millimeter-Wave Generation and Wireless Data Transmission Using a Dual-Mode Laser", IEEE Phot. Techn. Lett., vol. 12, (2000), p.1692-1694
10. K. Kato: "Ultrawide-Bandwidth High Frequency Photodetectors", IEEE Trans. Microw. Theory and Techn., vol.47 (1999) pp.1265-1281
11. G.A. Vawter, A. Mar, V. Hietala, J. Zolper, J. Hohimer: "All Optical mm-Wave Generation Using an Integrated Mode-Locked Semiconductor Ring Laser and Photodiode", IEEE Phot. Techn. Lett., vol.12 (1996), pp.1634-1637.
12. S. Donati, T. Tambosso: "Device for information transmission and/or reception by means of millimeters wave signals, corresponding module and method" Intl. Patent PCT/IT02/00414 (filed June 21, 2002)